(15) H. Collard, R. Hofstadter, B. Hughes, A. Johanson, M.R. Yearian, R. B. Day and R.T. Wagner: Phys. Rev. *138B*, 59 (1965); R.H. Dalitz and T.W. Thacher: Phys. Rev. Lett. *15*, 204 (1965); L.I. Schiff: Phys. Rev. *133*, B802 (1964).

(16) C.W. Akerlof; W.W. Ash, K. Berkelmann and M. Tigner: Phys. Rev. Lett. *14*, 25 (1965). In the MultiGeV region: A. A. Cone, K.W. Chen, J.R. Dunning Jr., C. Hartwig. N.F. Ramsey, J.K. Walker and Richard Wilson: Phys. Rev. Lett. *14*, *326* (1965).

(17) P. Panofsky, Hamburg Conference, June 1965.

(18) R. Cool, A. Maschke, L.M. Lederman, M. Tannenbaum, R. Ellsworth, A. Melissinos, J.H. Tinlot and T. Yamanouchi: Phys, Rev. Lett. *14*, 724 (1965); E. Amaldiana, G. Fidecaro, Helv. Phys. Acta. *23*, 93 (1950); Phys. Rev. *81* 339 (1951).

(19) The form factor $G(q^2)$ we are considering here is related to the cross section (differential versus the momentum transfer square) by (18):

$$\frac{d\sigma}{dq^2} = \frac{4\pi\alpha^2}{q^2} \frac{G(q^2)}{1 + q^2/4M^2} (1 - q^2/2Mp_o + ...)$$

and $G(q^2) = G^2_E + (q^2/4M^2) G^2_M$; α is the fine structure constant; G_E, G_M are the two known proton form factors; M the proton mass; p_o is the momentum of the incident muon.

(20) K.J. Barnes: Nuovo Cimento, *27*, 229 (1963).

(21) S.D. Drell: Ann. Phys. (N.Y.) *4*, 75 (1958).

(22) J.K. De Pagter, A. Boyarsky, G. Glass, J.I. Friedman, H.K. Kendall, M. Gettner, J.F. Larrabbee and Roy Weinstein: Phys. Rev. Lett. *12*, 739 (1964).

(23) G. Charpack, F.J.M. Farley, R.L. Garwin, T. Muller, J.C. Sens and A. Zichichi: Phys. Rev. Lett. *1*, 16 (1962).

(24) Results reported from the Stanford group at the present Conference.

(25) E. Wigner: Relativistic invariance and Quantum Phenomena. Rev. of Mod. Phys. *29*, 255, (1957).

(26) We are not considering, in this paper, the physics with colliding beams. Let's remember anyway that in these e.d. experiments the colliding beams of electrons shall have the greatest importance.

(27) R.B. Blumenthal, D.C. Ehn, W.L. Faissler, P.M. Joseph, L.J. Lanzerotti, F.M. Pipkin and D.G. Stairs: Phys. Rev. Lett. *14*, 660 (1965).

(28) S.D. Drell: Hamburg Conference, June 1965.

(29) A. Alberigi-Quaranta, M. De Pretis, G. Marini, A. Odian, G. Stoppini and L. Tau: Phys. Rev. Lett. 9, 226 (1962). J.K. Pagter, A. Boyarsky, G. Glass, J.I. Friedman, H.W. Kendall: Phys. Rev. Lett. *12*, 739 (1965). These results agree with quantum electrodynamics.

(30) I am grateful to R. Gatto for reminding this point. Of course the Compton effect at the smallest angles (which is the more interesting region) is either difficult or impossible.

(31) I don't intend here, of course, to discuss a choice between the proton and the electron machines, which is a much broader and difficult question. Consider for instance that the Protonsynchrotron can give a generous supply of photons through the π° decay. It is pleasent in itself to contemplate the internal consistency in the growth and advance of a research field.

STATUS OF DESIGN, CONSTRUCTION, AND RESEARCH PROGRAMS AT SLAC *

J. Ballam, G. A. Loew, R. B. Neal and the SLAC Staff

Stanford Linear Accelerator Center, Stanford University, Stanford, California (USA)

(Presented by R. B. Neal)

1. INTRODUCTION

Earlier planning and progress related to the Stanford Twomile Linear Accelerator were reported at previous conferences (1, 2, 3, 4). This report can be more definitive since it occurs at a time when the design of the accelerator and its auxiliary components and systems has been essentially completed and construction is well advanced. Completion of the accelerator will oc-

* Work supported by the U.S.A.E.C.

cur in 1966. The start of "shake-down" beam operations is scheduled for April 1966, and initiation of the physics program is scheduled for July 1966.

An overall plan view of the accelerator site showing the accelerator and Beam Switchyard housings, the research area, and the principal laboratories, shops and utility buildings is shown in Fig. 1. All of the structures shown are either completed or are in an advanced stage of construction.

Two of the 30 accelerator sectors were completed early and have been in operation with an electron beam since January 1965. Preliminary results have shown good correspondence with predicted performance. A more detailed account of these results is given in Section 3.

Planning of the initial research program and a brief description of the experimental equipment now being built is given in Section 4.

A review of the principal accelerator parameters is given in Table I. We will now turn our attention to the status of some of the most important components and subsystems.

TABLE I

Principal M accelerator specifications

	STAGE I	STAGE II
Accelerator length	10,000 feet	10,000 feet
Length between feeds	10 feet	10 feet
Number of accelerator sections	960	960
Number of klystrons	240	960
Peak power per klystron	6-24 MW	6-24 MW
Beam pulse repetition rate	1-360 pps	1-360 pps
R.f. pulse length	2.5 μsec	2.5 μsec
Electron energy, unloaded	11.1-22.2 GeV	22.2-44.4 GeV
Electron energy, loaded	10-20 GeV	20-40 GeV
Peak beam current	25-50 mA	50-100 mA
Average beam current	15-30 μA	30-60 μA
Average beam power	0.15-0.6 MW	0.6-2.4 MW
Filling time	0.83 μsec	0.83 μsec
Electron beam pulse length	0.01-2.1 μsec	0.01-2.1 μsec
Electron beam energy spread (max)	± 0.5%	± 0.5%
Multiple beam capability	3 interlaced beams with independently adjustable pulse length and current	
Accelerator vacuum	$<10^{-5}$ mm of Hg	10^{-5} mm of Hg
Operating frequency	2856 Mc/sec	2856 Mc/sec
Operating schedule	24 hrs/day	24 hrs/day

2. DESIGN AND FABRICATION STATUS OF PRINCIPAL COMPONENTS AND SUBSYSTEMS

a) Accelerator structure

The disk-loaded accelerator structure (5) is fabricated by a brazing technique in 10-foot sections of constant gradient design. Four of these sections are mounted on a 40-foot aluminum girder 24 inches in diameter, as shown in Fig. Waveguide feeds to successive sections are connected from opposite sides to compensate for coupler asymmetries. The 40-foot structure constitutes the basic accelerator module for purposes of construction instalation, provision of r.f. power, water cooling, alignment, and r.f. phasing. The aluminum girder serves dual functions as support for the accelerator and as a "light pipe" for accelerator alignment (see Section 2.j).

At the date of this conference, approximately 180 40-foot accelerator modules have been completed and installed in the Accelerator Housing. The remaining 60 modules will be installed by the end of this year.

b) Klystrons

Since design and fabrication of reliable high power klystrons to supply r.f. power to the accelerator was considered to be one of the most crucial tasks in the two-mile accelerator program, it was decided to undertake several development and manufacturing programs in parallel. Successful tubes meeting full specifications (21 MW peak power) have been produced by four outside companies and by SLAC (6). A group photograph of the five different tubes is shown in Fig. 3. All of these tubes are permanent-magnet-focused and are electrically and mechanically interchangeable.

c) Drive and phasing systems

The r.f. drive system consists of:

a) master oscillator providing 476-Mc/sec r.f. power;

b) a main booster amplifier which increases the 476-Mc/sec power to 17.5 kW cW;

c) a 3-1/8 inch-diameter main drive line two miles long which transmits the 476-Mc/sec power from the booster along the Klystron Gallery;

d) couplers at each 333-foot sector which remove ≈ 4 watts of power from the main drive line;

e) varactor frequency multipliers at each sector which multiply the frequency by 6 to 2856 Mc/sec;

f) a pulsed sub-booster klystron at each sector which amplifies the 2856-Mc/sec power from the varactor by 60 dB;

g) a 1-5/8-inch-diameter coaxial line which transmits power from the sub-booster klystron to the vicinity of each of the high power klystrons in the sector where the required amount (≈ 300 watts peak) is coupled off to drive the klystron.

The drive power is transmitted at 476 Mc/sec since the low loss (≈ 0.25 dB/100 feet) at this frequency in 3-1/8-inch coax permits transmission over a distance of two miles without the need for series boosters which, if used, would lead to phase shift and reliability problems.

The r.f. phasing system adopted (7) uses the phase of the electron bunches in the accelerator as a phase reference. It is based on the principle that the wave induced by the electron beam in an accelerator section is 180° out of phase with respect to the wave from a correctly phased klystron supplying power to the section. Phasing is accomplished automatically by sectors at the initiation of the operator. A programmer causes the phase of each klystron to be adjusted in turn, then passes to the next. The sequence of events is as follows: a) the klystron modulator trigger is delayed by ≈ 25 microseconds so that its r.f. output occurs after the beam pulses pass; b) the phase of the electron beam induced signal is compared to that of a cW reference signal from the output of the varactor multiplier and a calibrating phase shifter is adjusted to zero the detector in a microwave bridge circuit; c) the impressed wave from the klystron is then compared in phase with the cW reference signal and the phase shifter at the input to the klystron is adjusted to produce a zero in the phase detector circuit. This is the correct phase adjustment (within ±5°) for the klystron.

Fig. 1 - Site layout showing principal buildings and facilities.

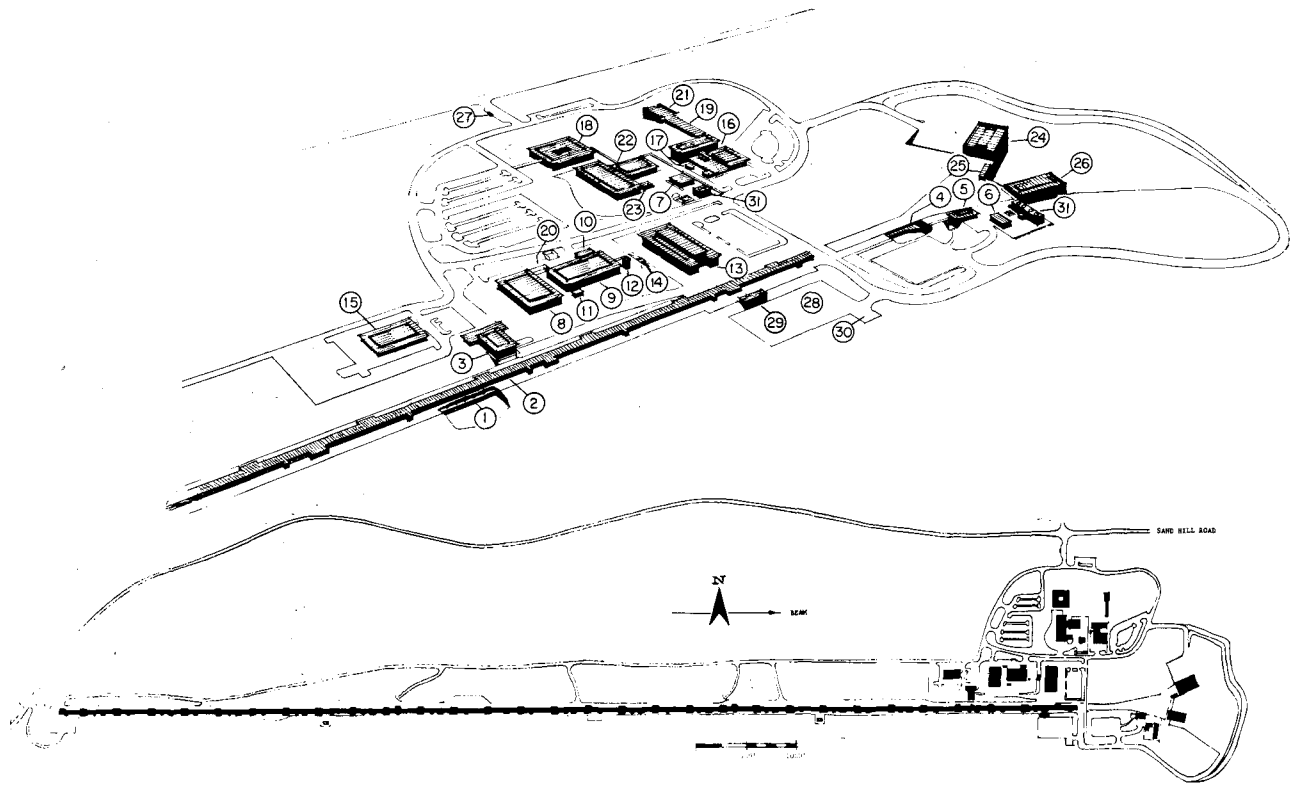

1 Accelerator housing
2 Klystron gallery
3 Control building
4 Beam switch yard
5 Data assembly
6 Sub station
7 Utility building "A"
8 Electronics and stores
9 Fabrication
10 Cleaning and plating
11 Sub station
12 Furnace building
13 Heavy assembly
14 Sub station
15 Construction office
16 Central laboratory
17 Sub station
18 Administration and engineering
19 Cafeteria
20 Lunch room
21 Auditorium
22 Test laboratory
23 Sub station
24 End station "A"
25 Sub station
26 End station "B"
27 Gate House
28 220 kV master sub station
29 switch house
30 60 kV sub station
31 Cooling tower

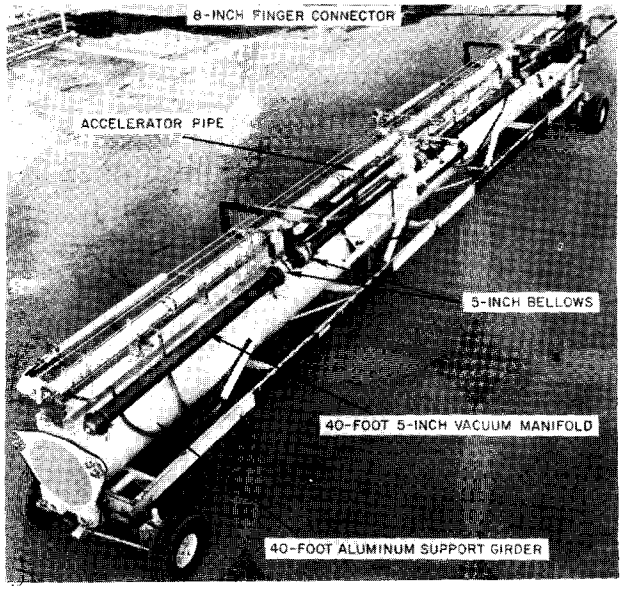

Fig. 2 - Basic 40-foot accelerator module consisting of four 10-foot sections mounted on a 24-inch-diameter aluminum girder. Entire assembly is shown on carrier system used for transport between fabrication shop and accelerator housing.

d) High power modulators

Each klystron amplifier is provided with a "line-type" modulator rated at 65 megawatts peak and 75 kilowatts average power, a pulse length of 2.5 microseconds, and a maximum pulse repetition rate of 360 pps. The pulse-forming network in the modulator is discharged through a single hydrogen thyratron capable of handling the entire peak and average power requirement. The voltage of the output pulses from the modulator is increased by a factor of 12 by means of a pulse transformer, and the resulting pulses at a voltage of 250 kV (maximum) are then applied to the associated klystron.

Each modulator is provided with a de-Q'ing circuit which compares the charging voltage of the pulse network during each charging cycle to a reference voltage. When the level of the charging voltage reaches the reference level, the energy stored in the charging transactor is dumped into a dissipative circuit by means of a silicon-controlled rectifier switch. This effectively clamps the charging voltage at the reference level and thus stabilizes the output pulses from the modulator to $\pm 0.1\%$ even in the presence of significant ($\approx \pm 5\%$) variations in the ac line voltage.

The pulse-forming network of the modulator is provided with tunable inductances which can be adjusted to produce an output pulse flat to $\pm 0.25\%$ for 2.5 microseconds.

e) Injector system

A diagram of the main injector is shown in Fig. 4. It is designed to inject a well bunched (5°) and well collimated beam of electrons into the accelerator. The electron gun which operates at 80 kV is of the triode type which permits the pulse length and beam current to be selected on a pulse-to-pulse basis from any of three predetermined sets of values. This feature of the injector, together with the ability to trigger the klystrons in the various sectors in time with or after the beam (or at various repetition rates), permits carrying on several simultaneous experiments in the research areas at different incident energies, pulse lengths, and intensities. The prebuncher consists of a velocity modulation cavity. The bunching section is a disk-loaded section 10 cm long in which the phase velocity is 0.75 c. It serves to reduce the phase spread by a factor of 2 (while doubling the momentum spread) and increases the beam energy to 250 kV. A 10-foot-long constant gradient accelerator section increases the energy to approximately 30 MeV. For phase synchronization, the pre-buncher, and 10-foot accelerator section are all driven by power from the same klystron, which is conservatively run at 1/2 to 2/3 of its power capability to give good life and stability.

The bunch monitor samples the harmonic content of the beam at the fundamental frequency, 2856 Mc/sec, and at the fifth harmonic by means of a pair of cavities. The difference between the power from the two cavities is proportional to the square of the bunch lenght (8).

Provision has been made for later installation of deflector plates to be driven at an r. f. subharmonic frequency to obtain a small number of widely spaced electron bunches.

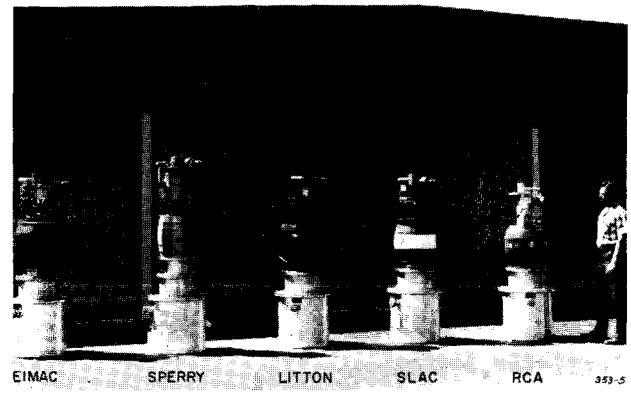

Fig. 3 - Klystron models manufactured by SLAC and by four commercial companies. All these tubes are mechanically and electrically interchangeable.

f) Positron source

A positron beams is desired at the 2/3 point along the accelerator length for injection into a proposed positron-electron storage ring and at the main experimental station at the end of the accelerator for positron scattering experiments. The positron beam will be created at the 1/3 point along the machine by inserting a converter and reversing the r.f. phase of the first 1/3 of the. accelerator. With 100 kW of incident electron beam power, it is predicted that approximately 2.5×10^{10} positrons per pulse can be accelerated in an energy band of about 1% and a transverse phase space of approximately 0.3 mc-cm.

The positron source system is shown in Fig. 5. Either of two separate radiators can be inserted into the beam. A radiator has a thickness of about 3.5 radiation lengths and consists of 5 to 10 layers of gold, silver, and copper with cooling water passages between. A « wand » radiator is provided for intermittent positron pulses at rates of one per second or less. It is a small target about 0.5 inches wide driven across the beam line on command in a time equivalent to about 9 machine pulses (at 360 pps). The center pulse of this group results in a positron pulse; the other 8 are caused to be blank by gating the main injector. All other pulses may be the electron beam, if desired. The second radiator is in the form of a rotating water-cooled wheel. It is used when continuous positron production is desired.

A magnetic lens system is used to improve the match between the source emittance and the accelerator phase space acceptance. The radiator is located in a 20 kG axial magnetic field which decreases rapidly to 2.4 kG about 2 feet downstream of the radiator and then remains constant for the next 25 feet. Acceleration begins 2.5 feet downstream of the radiator and the positron energy at 25 feet is about 75 MeV, at which point the solenoidal focusing is replaced by a series of 13 quadrupole triplets whose spacing increases with energy until this focusing system merges with the regular machine triplet system located at the end of each sector.

A pulsed r. f. deflector located downstream of the converter is used to produce an angular deflection of the positron and electron beams. Since the beams are 180° apart in phase, they are both deflected by the same angle; depending on which beam is needed, a magnetic dipole can then be used to restore the direction of either the positron or the electron beam to the axis while deflecting the other even farther.

g) Beam guidance and diagnostic equipment

To compensate for the earth's magnetic field and for stray ac and dc fields along the machine, parallel degaussing wires and concentric magnetic shielding are provided, reducing the average fields to $< 10^{-4}$ gauss (9). The degaussing currents are independently adjustable for each sector. The magnetic shielding material consists of 0.006-inch of moly-permalloy material which results in a local shielding factor of about 30 and an overall effective value of about 10, considering unavoidable gaps.

Beam monitoring, steering, and focusing devices are provided in a 10-foot drift section at the end of each 333-foot sector of the accelerator. The layout of a standard drift section is shown in Fig. 6. Equipment in this section consists of a quadrupole triplet, steering dipoles (X and Y), a phase reference cavity, beam position monitors (X and Y), a beam intensity monitor, a beam profile monitor, and a « beam scraper » (collimator). Triplets were chosen instead of doublets primarily on the basis of easier alignment tolerances (10).

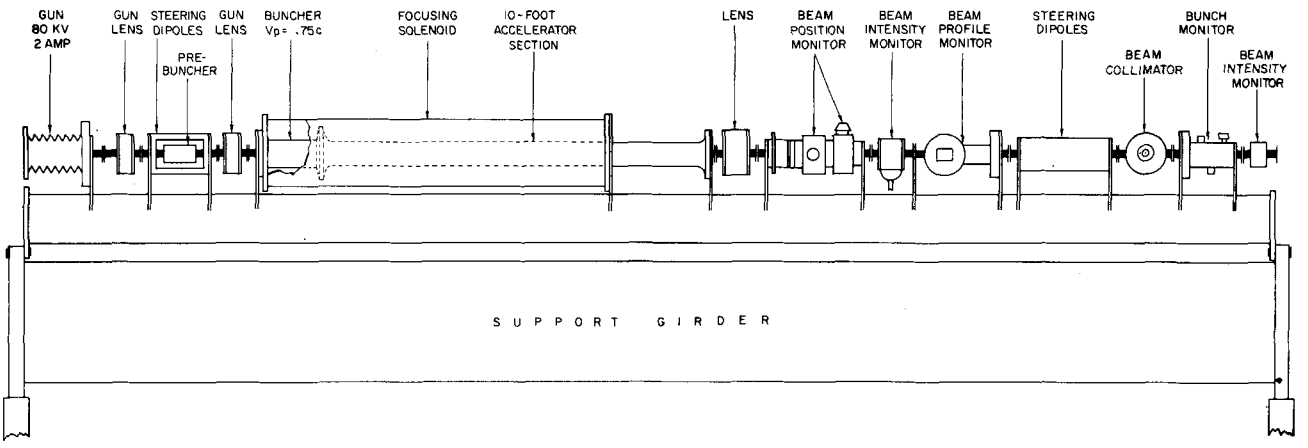

Fig. 4 - Profile view of injector.

The beam position monitors consist of two rectangular cavities which are excited in the TM_{120} mode by an off axis beam. Since the phase of the excitation depends on the direction of beam deviation from the axis, the sense of the deviation can be detected by comparing the phase of the wave from the beam position monitor cavities with the phase of the wave from the phase reference cavity which is excited in the TM_{010} mode (10). Beam positions accurate to < 1.0 mm from 30 such systems are presented at Central Control.

Several types of profile monitors are under consideration. One type uses a retractable 0.030-inch-thick quartz Cerenkov radiator and a TV viewing system. Another monitor under investigation utilizes a small metal bead which scans the beam aperture at a rapid rate. The intensity of X-radiation from this bead provides a measure of beam intensity at each point in the aperture.

h) Trigger system

Although the basic repetition of the accelerator is 360 pps, the trigger system permits operation of the various accelerator sectors and other subsystems in a very flexible manner so that up to six beams having distinct energies, currents ,and destinations in the research area can be programmed. The repetition rates of these beams can be adjusted to be any value between 1 and 360 pps. The trigger system is illustrated in Fig. 7. Clock pulses at a 400 V level and 360 pps are sent over the entire two-mile length along a single 1-5/8. inch-diameter coaxial cable. A small amount of power is removed from the main line by means of couplers at each station (injector, accelerator sector, positron source, etc.) and is sent to the local trigger generator. A gating pulse is sent to each local trigger generator from the pattern generator in Central Control. Since the timing precision ($\approx$ 25 nanoseconds) is inherent in the clock pulses, the gating pulses do not have to be very precise and can be transmitted on ordinary wire pairs.

In Fig. 7, the pattern generator pulses are shown gating the clock pulses admitted to the klystron modulators of each sector. If a particular sector is not to contribute to the energy of a particular beam, the pattern gating signal causes the modulators to be triggered approximately 25 microseconds late, after the beam pulse has been transmitted through the sector. In other arrangements, the pattern signals may cause a particular sector to pulse at lower repetition rates, such as 60, 120, and 180 pps.

i) Vacuum system

The all-metal high vacuum system (11, 12) capable of maintaining the accelerator and waveguide

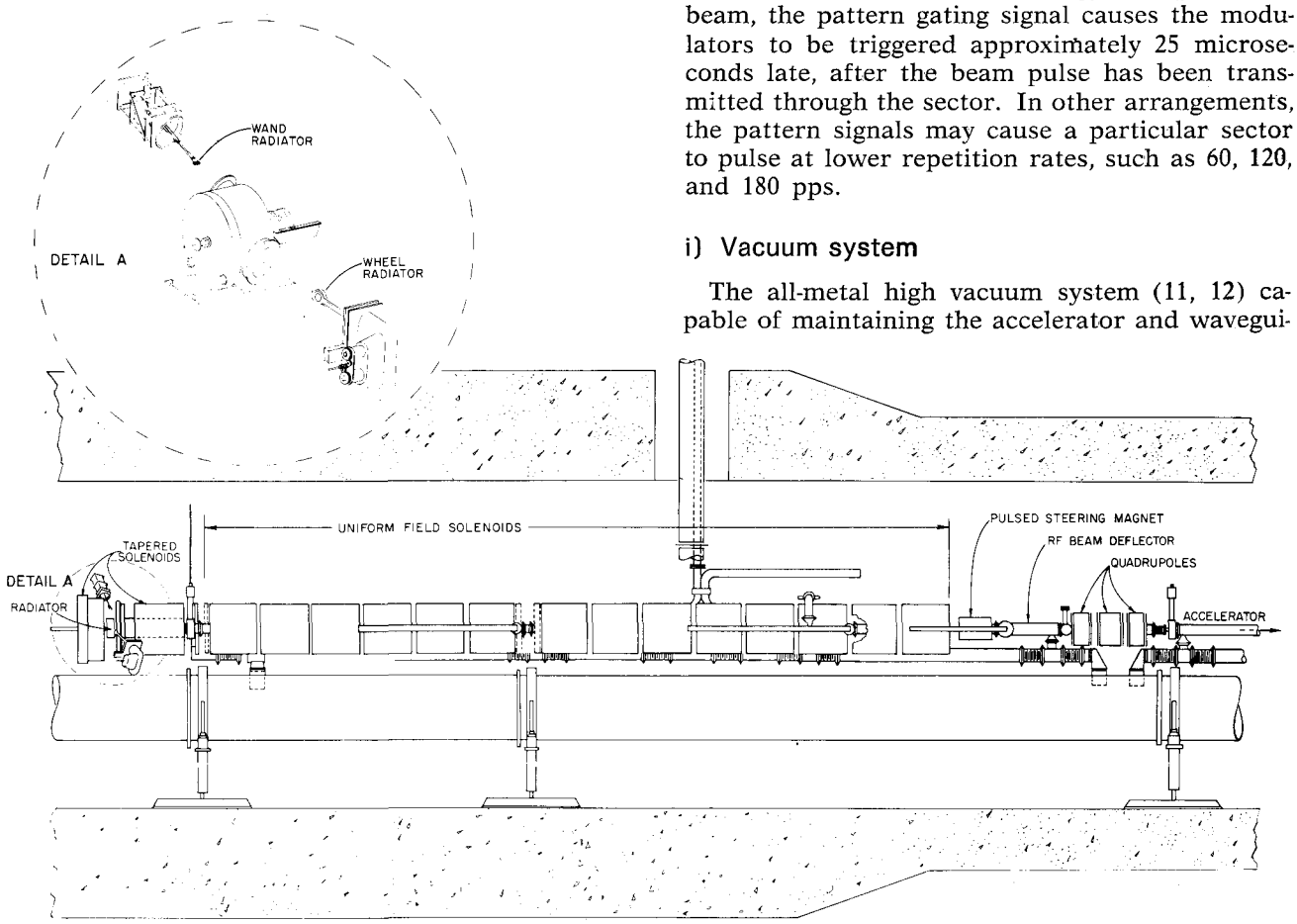

Fig. 5 - Positron source.

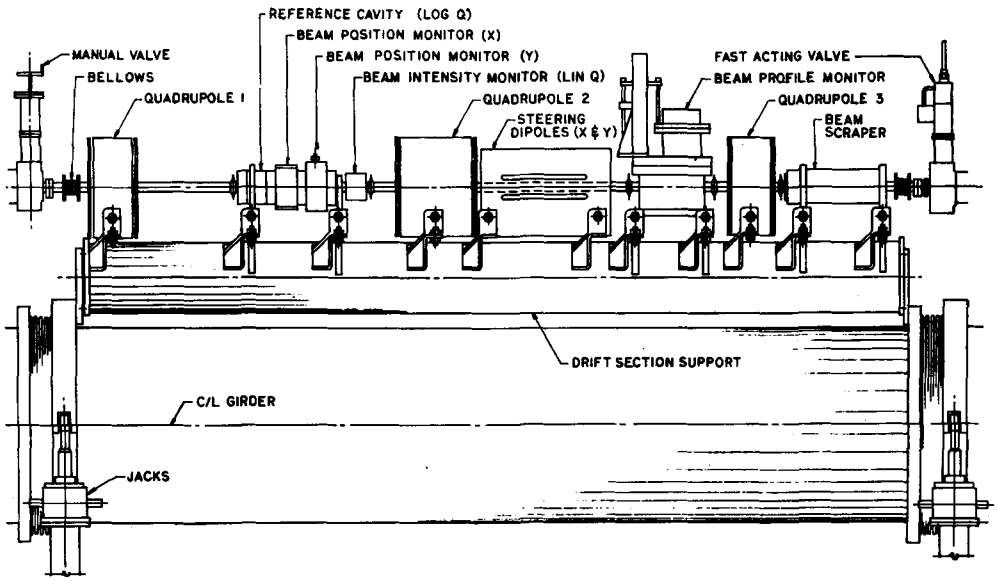

Fig. 6 - Standard drift section located at end of each 333-foot sector.

des at $< 10^{-6}$ torr is shown schematically in Fig. 8. One such system is provided for each 333-foot sector. Four 500 liter/second getter-ion pumps located in the Klystron Gallery evacuate the accelerator and waveguides through interconnecting stainless steel manifolds. Pumps can be removed for servicing without interference with accelerator operations by closing the associated 6-inch valve. Similarly, individual klystrons can be replaced by closing the 3-inch valve connecting it to the pumping manifold and the waveguide vacuum valve in its output r. f. system.

Separate pumping systems are provided for rough-pumping the accelerator, for the 24-inch "light pipe", and for the Beam Switchyard.

j) Alignment system

Each of the 40-foot support points of the accelerator is aligned with respect to a straight line defined by two end points. One of the end points is a laser light source located at the end of the accelerator near the Beam Switchyard and the other end point is a slit with a photomultiplier detector located upstream from the main injector. The laser light source provides a beam of light which is transmitted through the 24-inch aluminum support girder. The girder ("light pipe") is evacuated to a pressure of about 10 microns to reduce refraction due to temperature gradients in the residual gas. At each 40-foot support point, a retractable Fresnel target (13), as shown in Fig. 9, images the light source on the detector. The transverse location of the image indicates the deviation of the target from its correct position. The adjustable jacks at the corresponding support point can be adjusted to bring the target into correct alignment. The correct angular rotation of the accelerator is assured by the use of precision level devices. Experiments have shown that the system described should be able to align the accelerator to $\pm$ 0.5 mm.

k) Beam switchyard

A layout of the Beam Switchyard is shown in Fig. 10. This is a large two-level underground structure (14) located under 40 feet of concrete and earth for radiation shielding purposes. The beam path itself is located on the lower level. The upper level contains utility runs, instrumentation and control alcoves, cranes, service cars, and other equipment required in conjunction with the main beam handlingh equipment in the lower level. Parameters of the Beam Switchyard transport system are shown in Table II.

The unsually high power ($\approx$ 1 MW in Stage I) carried by the incident beam has imposed very difficult problems in the design of the beam handling equipment. A typical example of a device capable of handling these large beam powers is the 16-foot-long adjustable aluminum slit shown in Fig. 11. Two in-line slits of the type shown, with the second rotated 90° about its axis with respect to the first, are used as an adjustable collimator at the beginning of the Beam Switchyard.

A small digital process control computer (IBM 1800) will be used in the control system of the Beam Switchyard for the following purposes:

1. The computer will read data from punched cards and send control information to the regulators in the magnet power supplies where a digital-to-analog converter will convert the digital in-

TABLE II

Parameters for the transport system of the SLAC beam switchyard

	Electron-Photon Area	Secondary Beam Area
Maximum energy	25 GeV	25 GeV (expandable to 40 GeV)
Input conditions		
Beam radius	0.3 cm	0.3 cm
Angular divergence	$< 10^{-4}$ rad	$< 10^{-4}$ rad
Energy spread	<2%	< 6%
Total bending angle	24.5°	12.5°
Resolution	0.1%	0.2%
Dispersion at slit	0.15%/cm	0.3%/cm
Isochronicity (at 2856 Mc/sec)	< 10°	< 10°
Achromatic	Yes	Yes
Final beam size	≈ 2 mm	≈ 2 mm

formation to an analog reference voltage. Slits and collimators will be adjusted in a similar way.

2. When desired by the operator or experimentalist, data determining the parameters of a particular beam will be printed out from the computer memory for record, together with auxiliary information.

3. About 100 signals from various sources will be scanned every accelerator pulse (1/360 second) and about 600 signals will be scanned at a slower rate. The computer will detect, identify, and print out the time and date of any changes in the interlock and status signals in proper sequence.

3. PRELIMINARY TESTS IN SECTORS 1 AND 2

a) Purpose and conditions of early tests

The beam and systems tests whose results are given in this section were carried out on Sectors 1 and 2 between January and July, 1965. These tests have reinforced our confidence in the basic design and have pinpointed some desirable improvements which have been incorporated in the rest of the machine. The tests were performed before the final injector described in 2.e above was in place. The simplified and optically somewhat inferior injector which was used consisted of an oxide gun of an early design, a prebuncher, and two lenses. To evaluate the quality and energy of the beam, two special beam analyzing stations were installed, one at the 40-foot point, shown in Fig. 12, and the second at the end of Sector 2. Each station consists of a spectrometer magnet, a beam dump, an array of secondary emission monitor foils to obtain a dynamic energy spectrum display, and other beam guidance instrumentation, similar to that included in the regular accelerator drift sections. Both these stations have been found so useful that they will be permanently incorporated in the machine. The alignment of the two sectors was performed by means of the stretched wire technique and spirit levels, since the laser system was not yet available. Temporary instrumentation and control was centralized in the Sector 2 alcove. Communications over the 666-foot length were assured by means of the advanced equipment shown in Fig. 13.

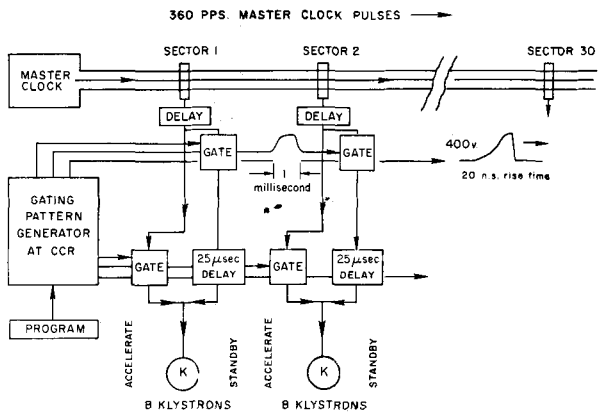

Fig. 7 - Trigger system block diagram.

b) Results of beam operation

The first electron beam in the accelerator was obtained at 02:15, January 6, 1965, at the 40-foot beam analyzing station. By January 27, 1965, a five-milliampere peak current beam with an energy of 620 MeV was obtained at the end of Sector 2. From then until June 17, 1965, the two-sector machine was operated and tested on a regular day-to-day basis. The highest energy of 1.45 GeV was obtained with all 18 klystrons (the first 3 installed in the Stage II configuration) operating at an average peak voltage of 240 kV and a peak power of about 20 MW. This operating level would yield 680 MeV per sector or more than 20 GeV for the complete machine. These results indicated that the predicted disk-loaded waveguide efficiency given by the relation

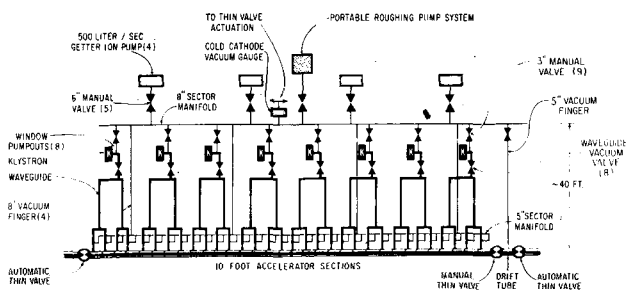

Fig. 8 - Vacuum system schematic for one 333-foot sector.

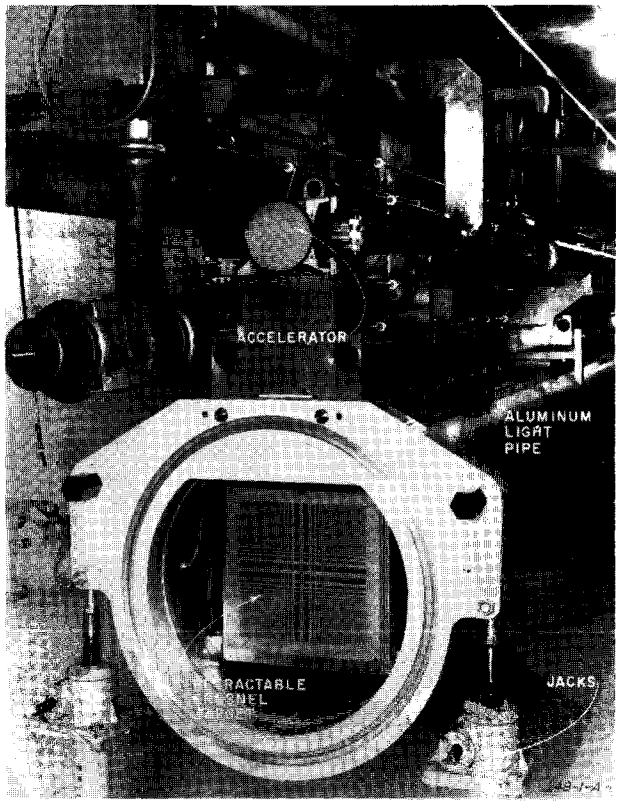

Fig. 9 - End of 40-foot girder showing retractable Fresnel target in position inside light pipe.

Fig. 10 - Plan view of Beam Switchyard showing principal components and cross section of housing at different points. AP - Pulsed Steering Magnet; C - Collimator; B - Bending Magnet; PM - Pulsed Magnet; D - Beam Dump; Q - Quadrupole; SL - Energy Defining Slit; A - dc Steering Magnet.

$$E\left(\frac{\text{MeV}}{\text{Girder}}\right) = 19.9\sqrt{P\left(\frac{\text{MW}}{\text{Klystron}}\right)}$$

was quite conservative and that the tuning of the four-way rigid rectangular waveguide runs is being done correctly.

The energy spectrum of the machine was studied extensively and recorded under a wide variety of conditions to measure the effects of phasing, frequency tuning, water temperature adjustments, changes in repetition rate, beam loading and trigger timing. Figure 14 shows the results of a typical experiment. In this case, spectrum 1 was obtained at the end of Sector 2 after the frequency had been adjusted from 2855.9 to 2856.0 Mc/sec without rephasing. Specturm 2 was then obtained after phasing, and spectrum 3 somewhat later, after rephasing a second time. These curves illustrate the increase in energy obtained and the reproducibility of the automatic phasing operation as well as the overall stability of the machine. The apparent negative current swing exhibited by the spectrum still remains somewat of a mystery although its origin lies in scattered and secondary electrons produced when the spectrum peak intercepts the wall of the spectrometer vacuum envelope.

The effect of beam loading is illustrated in Fig. 15, which shows a three-dimensional plot of current pulse profiles as a function of time and energy. Each profile was obtained by taking a photograph of the current pulse picked up on a secondary emission foil in the analyzed beam at the end of Sector 2 for a given magnet current setting.

Considerable experience was gained in making use of the beam guidance system to steer and focus the beam. The special steering dipoles

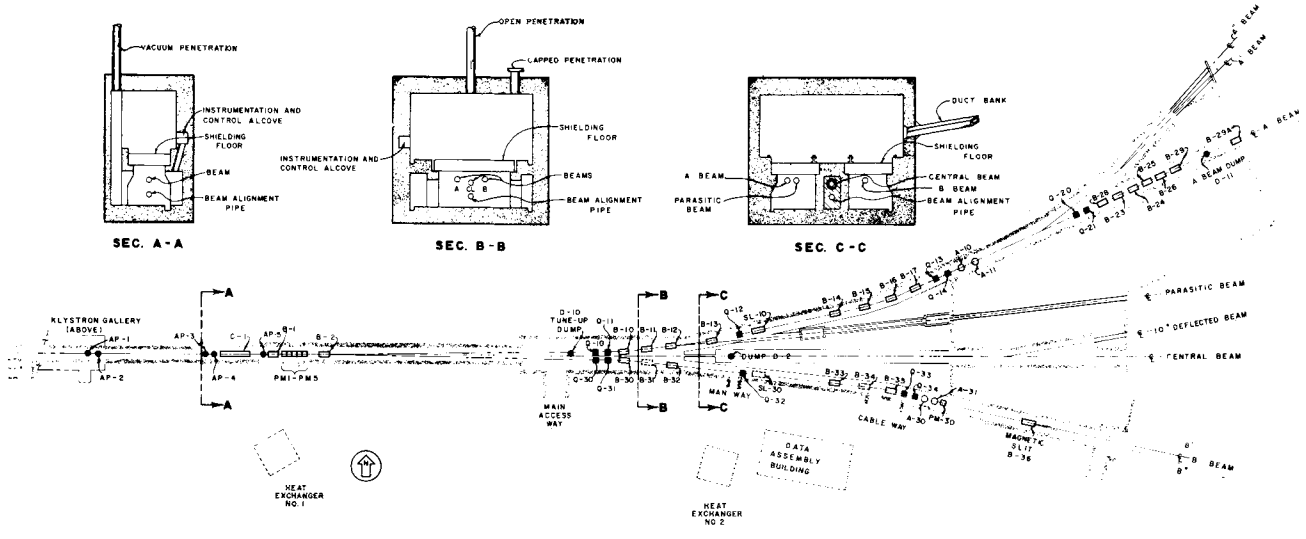

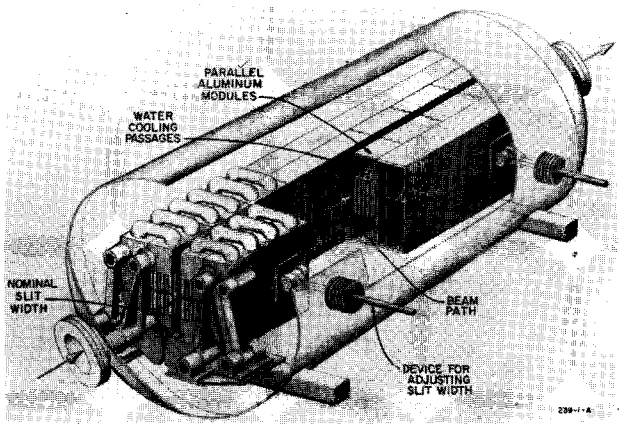

Fig. 11 - High power energy-defining slits.

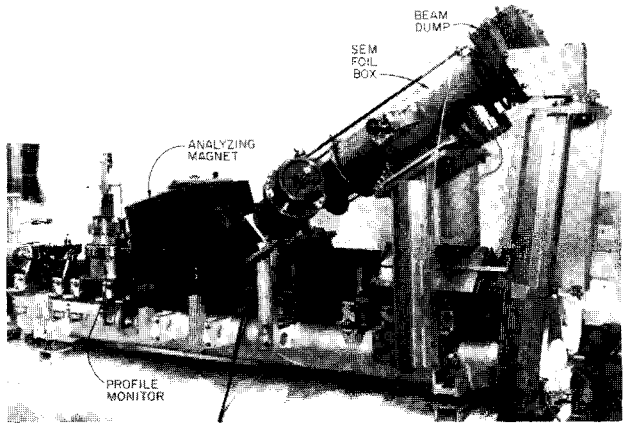

Fig. 12 - Beam analyzing station at 40-foot point.

installed in Sector 1 to compensate for the horizontal coupler asymmetry (10) (not compensated for in this sector by waveguide feed alternation) were found very useful. In Sector 2, such dipoles were not necessary although an unexpected asymmetry in the vertical plane was found to deflect the beam somewhat when a particular klystron accidentally recycled. This effect is not serious, but still remains to be explained. The quadrupole triplets appeared to perform correctly and their effect on beam transmission and beam shape was studied carefully by means of the Cerenkov radiation quartz profile monitors. Some difficulty was experienced with these because of saturation of the TV display. Also, careful use had to be made of the beam position monitors in order to steer the beam through the center of the quadrupoles. Otherwise, steering and focusing could not be decoupled and the procedure to obtain an optimum beam converged extremely slowly. When the beam could not be found, the so-called "PLIC" (Panofsky's Long Ion Chamber), in spite of the poor resolution obtainable over two sectors, turned out to be extremely useful in detecting major radiation areas along the machine. The magnetic shielding and degaussing system appeared to be satisfactory.

On the whole, overall beam transmission still left something to be desired. Substantial improvements are expected when the machine gets tested with the final injector.

The feasibility of programming different beams on a pulse-to-pulse basis by means of the trigger system was verified by a variety of experiments. Although it will not be known until the machine is complete whether multiple energy beams can be steered through the two-mile length with *dc* steering dipoles alone, the generation of beam patterns seems to work nicely. For example, the following experiment was made. All klystrons were operated at 360 pps and the gun, pulsed at 60 pps, was successively switched through the six phases of 60 pps making up 360 pps. No beam shape or position change could be detected on either the profile or the position monitors.

c) Individual systems performance

It is beyond the scope of this report to describe all the tests and measurements made on all individual accelerator systems. Some of the highlights of the test results and observations are given below.

The r.f. drive system, from the master oscillator at 476 Mc/sec to the high power klystrons, operated quite reliably. Some phase drifts as a function of ambient temperature were discovered and a retrofitting program to improve the anchoring and insulation of the drive lines is in progress.

The automatic phasing system appeared to operate well and after some initial adjustments and improvements it was capable of phasing a sector in one minute. However, the thermionic diodes used in this system as well as in the beam intensity and position monitor system still suffer from short- and long-term drift over the wide dynamic range required (50 dB). Circuit changes are being studied to reduce this effect.

Klystron performance in Sectors 1 and 2 has been quite good. Over a period of one year with an initially low number of "r.f.-on" hours but a progressive increase to approximately four 8-hour shifts per week, only three tubes failed in the gallery and nine other tubes were removed because of ancillary equipment failure. The modulators, after an initial "Darwinian" elimination of weak pulse capacitors, thyratrons and relays, operated very reliably.

The amplitude and phase stability of klystron r.f. output within a pulse and pulse-to pulse has

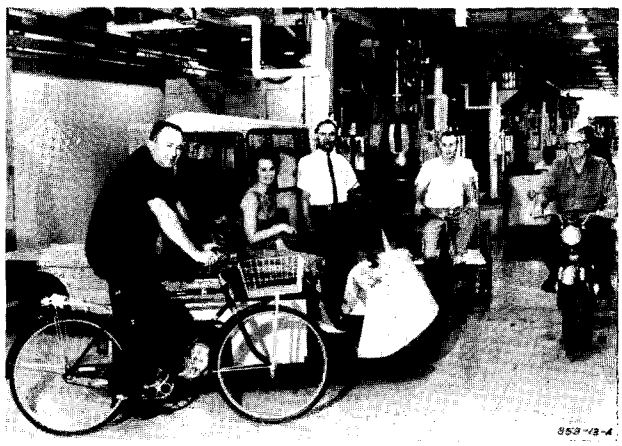

Fig. 13 - Advanced communications systems in Klystron Gallery.

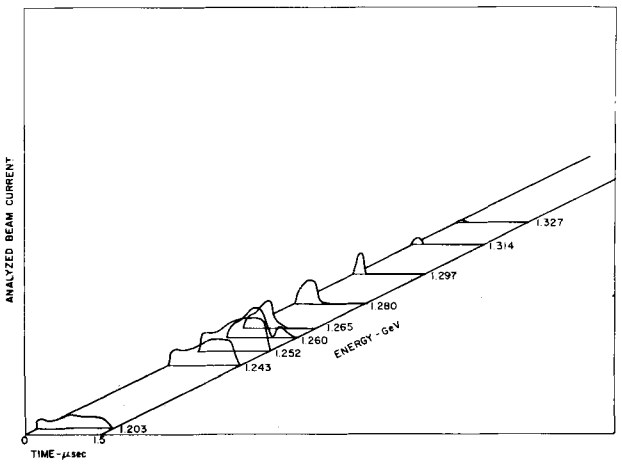

Fig. 15 - Beam current vs time and energy at 666-foot point.

been found to be very satisfactory. Fig. 16 shows examples of amplitude and phase stability for two klystrons. Envelopes are shown at both input and output of an accelerator section to illustrate the effect of the pass-band nature of the accelerator structure. Good correlation is seen between phase modulation ($\approx$ 1.5 electrical degrees) and voltage ripple (less than 1/2%). Pulse-to-pulse phase jitter was of the order of tenths of one degree.

Klystron recycling in Sector 1, which caused the beam spot to move because of coupler asymmetry, was still somewhat excessive. However, the frequency of recycling could generally be reduced to a negligible number ($\approx$ one per hour) by operating at a conservative beam voltage, around 215 kV. After a few hours of continuous operation and steady outgassing, the accelerator ran very reliably. During a final endurance run, the two sectors operated for an eight-hour period with only 4 or 5 individual klystron "kickouts".

The vacuum system operated with relatively few problems. Only one major leak developed after the initial pumpdown period. The two sectors were let up to nitrogen on several occasions. A combination of mechanical and cryopumps was used do rough down the system to 2×10^{-4} torr. This operation took about 70 minutes. The subsequent pumpdown by means of getter-ion pumps to 10^{-6} torr in the 8-inch manifold could be achieved in 10 minutes. To get to 10^{-7} torr scale took about 24 hours.

The water cooling system, in particular the accelerator structure cooling loop, operated very well and except for one major drift was stable within a fraction of 1°F.

The power system and in particular the variable voltage substations appeared to operate reliably. As predicted, it was found that at maximum repetition rate and power, each klystron consumed approximately 100 kW.

The major system which remains to be tested is the Instrumentation and Control System, in particular those parts involving transmission and decoding of information over the two-mile length. These subsystems are just being received. The installation of equipment in the Central Control Building has begun.

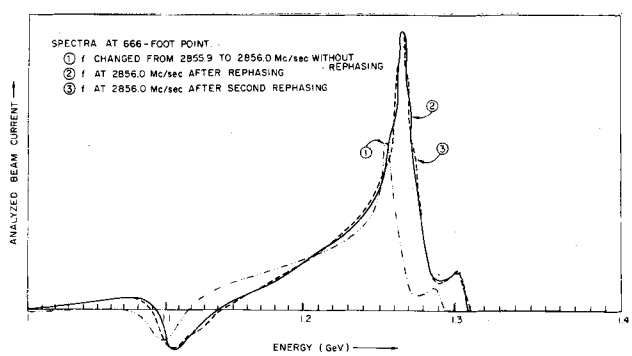

Fig. 14 - Effect of phasing and frequency tuning on energy spectrum.

4. INITIAL RESEARCH PROGRAMS

The laboratory is planning an extensive research program designed to take advantage of the unique features of the linear accelerator and scheduled to be ready at the time the accelerator is available for this purpose. The first experiments will explore the properties of electron, muon, and photon interactions with protons, using a wide range of experimental methods involving both counters and visual techniques. This section will outline briefly the main physics goals of the program and describe in somewhat more detail the experimental apparatus which is under design and construction.

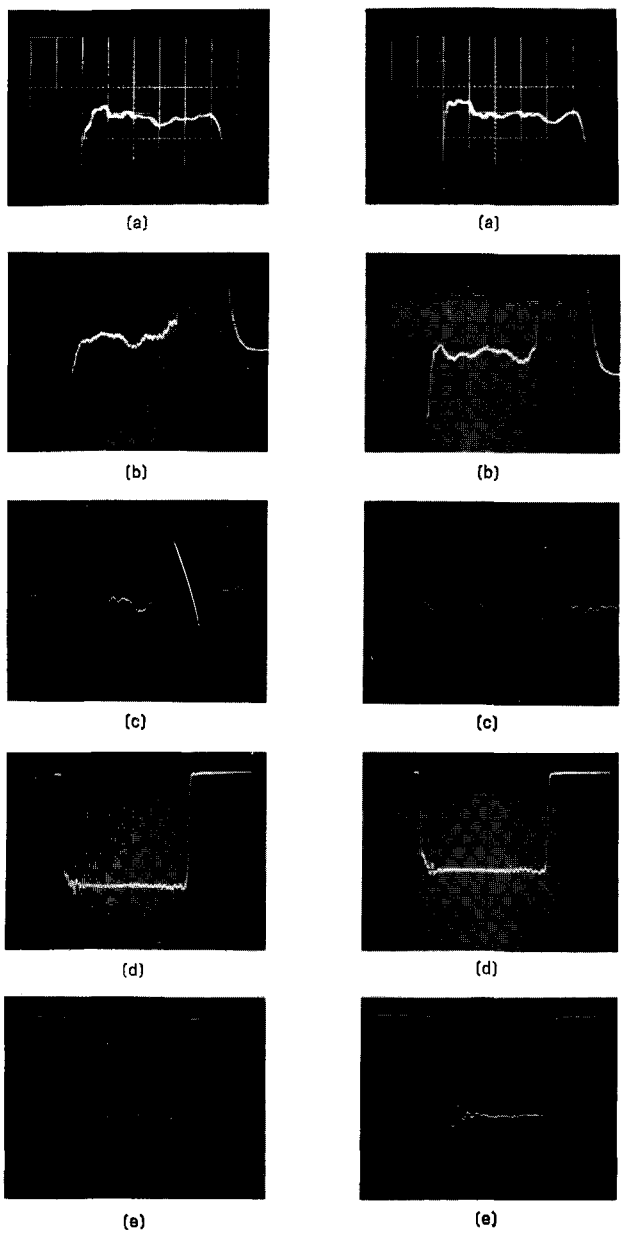

Fig. 16 - Examples of performance of two klystrons. (a) Klystron beam voltage. (1 div $\rightarrow \Delta V/V = 1\%$); (b) Phase at of accelerator section; (d) R.f. envelope at output of klystron; (e) R.f. envelope at output of accelerator section.

a) Physics program

1. *Elastic positron and electron scattering.*

The cross section for elastic scattering of electrons as a function of four-momentum transfer will be studied to values as large as $q^2 = 500\ F^{-2}$ (units of inverse fermi squared). The primary objectives are threefold: first, to investigate whether or not anomalies exist in quantum electrodynamics via small angle scattering of the 20 GeV electrons; second, to find out whether or not two-photon exchange plays a role in the scattering process by comparing positron and electron scattering at the same momentum transfer; and third, to measure the electric and magnetic form factors out to very large values of momentum transfer via large-angle scattering.

2. *Inelastic electron-scattering*

By examining the recoil electrons from inelastic collisions with protons, one can study photoproduction cross sections by virtual, monoenergetic, polarized photons of variable (spacelike) mass. Great precision is needed in measuring the momentum and angle of the electron so as to provide recognition of structure in the recoil momentum spectrum over the general background. These processes will be studied with magnetic spectrometers.

3. *Photoproduction processes*

These divide themselves into three main categories: electromagnetic pair production of any particle having either charge or magnetic moment; peripheral production in accordance with a Drell-like process; photoproduction from the point of view of electrodynamic multipoles. In all of these processes the production of resonances such as have been seen in the strong interactions will be studied. The techniques to be used involve

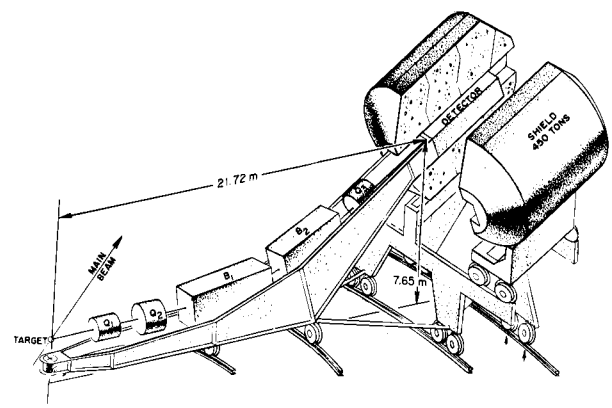

Fig. 17 - 8-GeV/c spectrometer.

Fig. 18 - 20-GeV/c spectrometer.

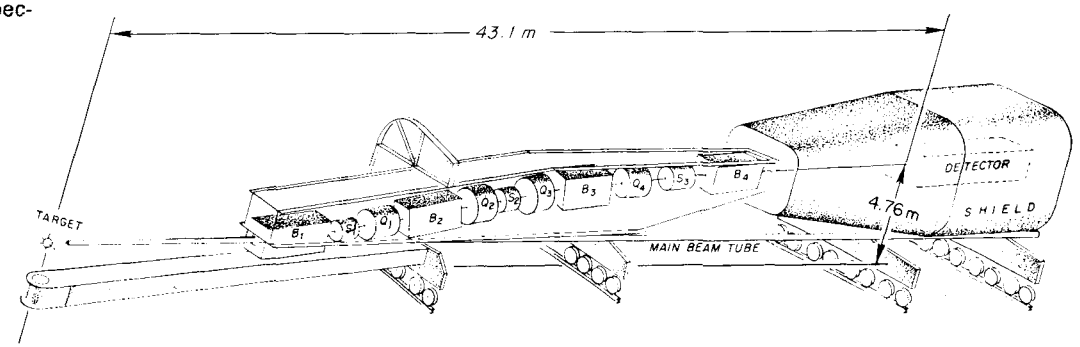

the magnetic spectrometer, the streamer-type spark chamber in a large-volume magnetic field, and the hydrogen bubble chamber. A survey of pion, kaon and anti-nucleon beams will also be done with the 20 GeV spectrometer.

b) Experimental apparatus

The large pieces of apparatus now being designed and procured by the various research groups are:

1. A 20 GeV/c magnetic spectrometer and counting system.
   An 8 GeV/c magnetic spectrometer and counting sistem.
2. A large-volume magnet for use with streamer and conventional spark chambers.
3. A photon channel for bremsstrahlung beams with end points up to 20 GeV.
4. A one-meter-diameter hydrogen bubble chamber.
5. A photon channel for monochromatic photons up to 10 GeV.
6. A muon channel for the formation of mu beams up to 12 GeV/c.
7. A 3 GeV electron-positron storage ring design only--- not yet authorized).
8. A large-volume streamer spark chamber.

Items 7 and 8 are being described elsewhere in the conference.

1. *Spectrometers*

The spectrometers are designed to do physics in the following areas:

a) elastic electron and positron scattering from nucleons;

b) inelastic electron scattering;

c) photoproduction experiments;

d) quantitative survey of secondary beams.

The specifications of the spectrometers are given in Table III. Notice that the momentum resolution and acceptance are matched to the transmission of the main electron beam through the Beam Switchyard show in Table II. This, coupled with the specified angular resolution, allows a

TABLE III

Specifications of SLAC 8 GeV/c and 20 GeV/c spectrometers

Momentum (max)	20 GeV/c	8 GeV/c
Momentum resolution	±0.05%	±0.05%
Solid angle acceptance	10^{-4} ster.	10^{-3} ster.
Momentum acceptance	±2%	±2%
Angular resolution	0.3×10^{-3} rad	0.3×10^{-3} rad
Angular range (production angle)	$\pm4.5\times10^{-3}$ rad	$\pm8\times10^{-3}$ rad
Azimuthal angle	$\pm8\times10^{-3}$ rad	$\pm30\times10^{-3}$ rad
Maximum target length (projected)	3 cm	10 cm
Minimum angle at which beam will miss instrument	≈ 3°	≈ 12°

Fig. 19 - Model of arrangement of spectrometers.

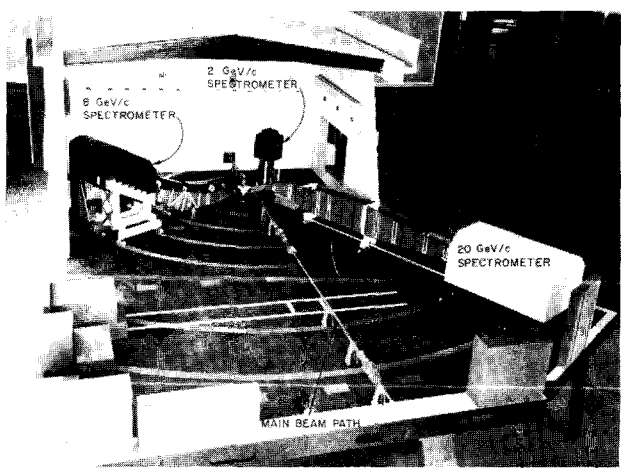

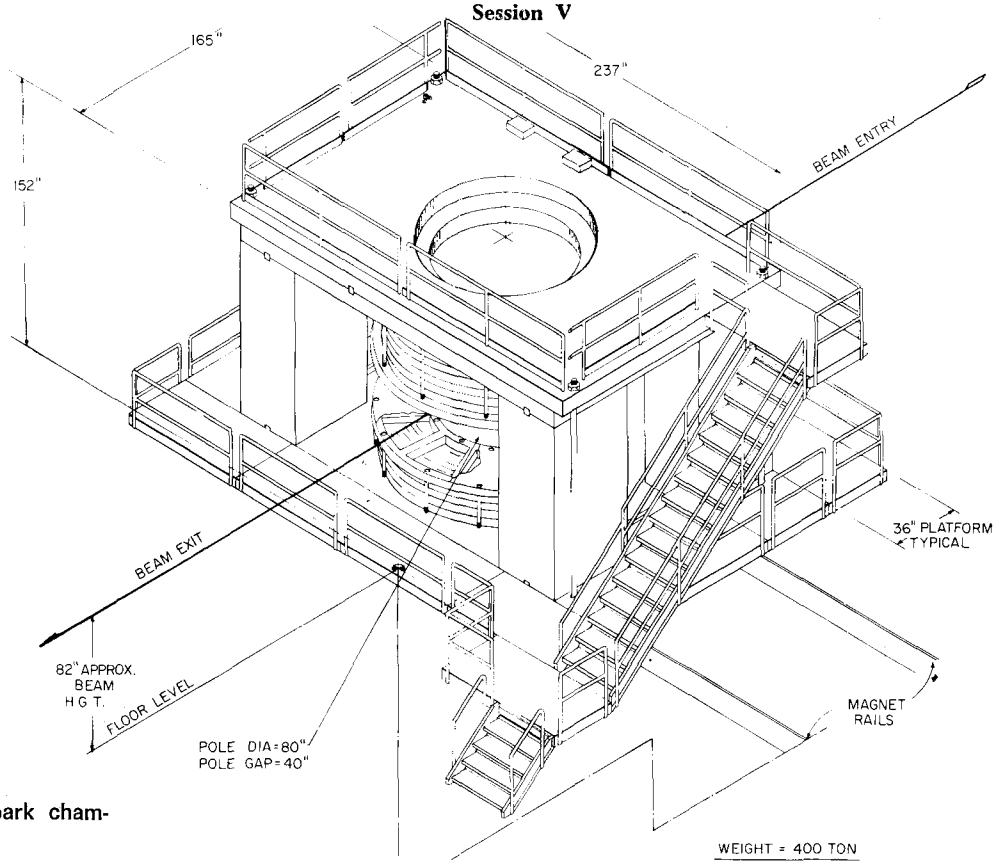

Fig. 20 - Spark chamber magnet.

kinematical distinction between the two processes:

$$[a] \quad e + p \rightarrow e + p$$

$$[b] \quad e + p \rightarrow e + p + n\pi^0 \quad n \geq 1$$

The overall dimensions and layout of the spectrometers are shown in Figs. 17 and 18. They are designed so as to disperse the momenta vertically and provide a line-to-point focus horizontally. There is thus a plane in the exit space in which each point of the plane represents a given set of p and θ. A hodoscope of very small scintillators is placed in this plane with its ouptut connected to an SDS 9300 computer. In this way it is hoped for most applications to replace coincidence counting with a high degree of spatial resolution. Cross sections as low as 10^{-37} cm^2 will be measured.

These two instruments will cover the solid angle in the center-of-mass system of the colliding particles with the exception of the very backward angles near 180°. The experimental area is designed so that a smaller ($\approx$ 2 GeV) spectrometer may be added to cover the backward region with a minimum of interference with the other two.

All three spectrometers would rotate around a common pivot, as shown in Fig. 19, and any pair can eventually be arranged to operate in coincidence. A discussion of the theory of the spectrometer design has been given by Panofsky (15).

TABLE IV

Magnet parameters

Gap height	1 m
Pole diameter	2 m
Turns per pole upper lower	297 or 231 165 or 231
Coil ID	2.25 m
Coil OD	3.62 m
Number of turns per pancake	16½
Number or pancakes upper pole lower pole	18 or 14 10 or 14
Hydraulic passages per double pancake	2
Conductor dimensions	(3.8×4.6) cm^2
Diameter of cooling hole	2.3 cm
Conductor cross section	13.2 cm^2
Magnet resistance incl. loads: (50°C) (100% ICAS) (60°C) (100% ICAS)	 $6.2\times10^{-2}\,\Omega$ $6.5\times10^{-2}\,\Omega$
Water flow at 6.6 MW	740 GPM
Temperature rise at 6.6 MW and 740 GPM	30.4°C
Pressure drop at 740 GPM	210 psi
Water flow at 8 MW	831 GPM
Temperature rise at 8 MW and 831 GPM	33°C
Pressure drop at 831 GPM (return pump required)	260 psi
Iron weight (no upper pole) (two poles)	370 tons 419 tons
Copper weight	56 tons

2. *Spark chamber magnet*

The basic purpose of this instrument is to study photoproduction processes using a relatively low intensity beam and a very large solid angle for detection. Typical reactions to be studied are:

$\gamma + p \rightarrow 3$ charged particles

$\rightarrow$ one charged particle and two neutral V's

$\rightarrow$ odd number of charged particles > 3.

The above can be accomplished by a simple trigger system together with the spark chamber in the magnetic field. In all these cases only the direction of the incident photon must be known accurately.

With more elaborate counter systems (especially those that can distinguish masses) and additional spark chambers to convert π° gamma rays, more complicated final states may be examined.

Further studies involving mu mesons are planned for this apparatus. Typical reactions are

$$\mu + p \rightarrow \mu + p + \pi^+ + \pi^- \text{ and } \mu + p \rightarrow \mu + p + \pi^\circ.$$

In this case a missing mass may be calculated since the momentum and direction of the incoming mu are defined. Under favorable circumstances cross sections down to 10^{-32} cm^2 should be measurable with this instrument.

A drawing of the magnet is shown in Fig. 20. It is designed to operate at 15 kG with 5.8 megawatts input. A unique feature is the flexibility of assembly. It can be assembled in any one of three configurations: no poles, one pole, or two poles. The basic dimensions are given in Table IV. Note that with increased water flow the magnet could be run at 8 megawatts.

The main feature of the configuration is to allow for arrays of triggering counters covering a large solid angle to be placed downstream of the target. Note also that right angle as well as conventional stereo pictures can be taken. In order to get a reasonable field over such a large volume, a decided sacrifice in uniformity had to be made. In some congurations a variation of as much as 30% exists. Computer programs for point-to-point evaluation of the field are being written.

An interesting model of this magnet was made and was scaled in ampere-turns as well as iron dimensions. This was accomplished by pulsing the magnet from a capacitor bank. This model was 1/10 scale and made of 0.014-inch lamina-

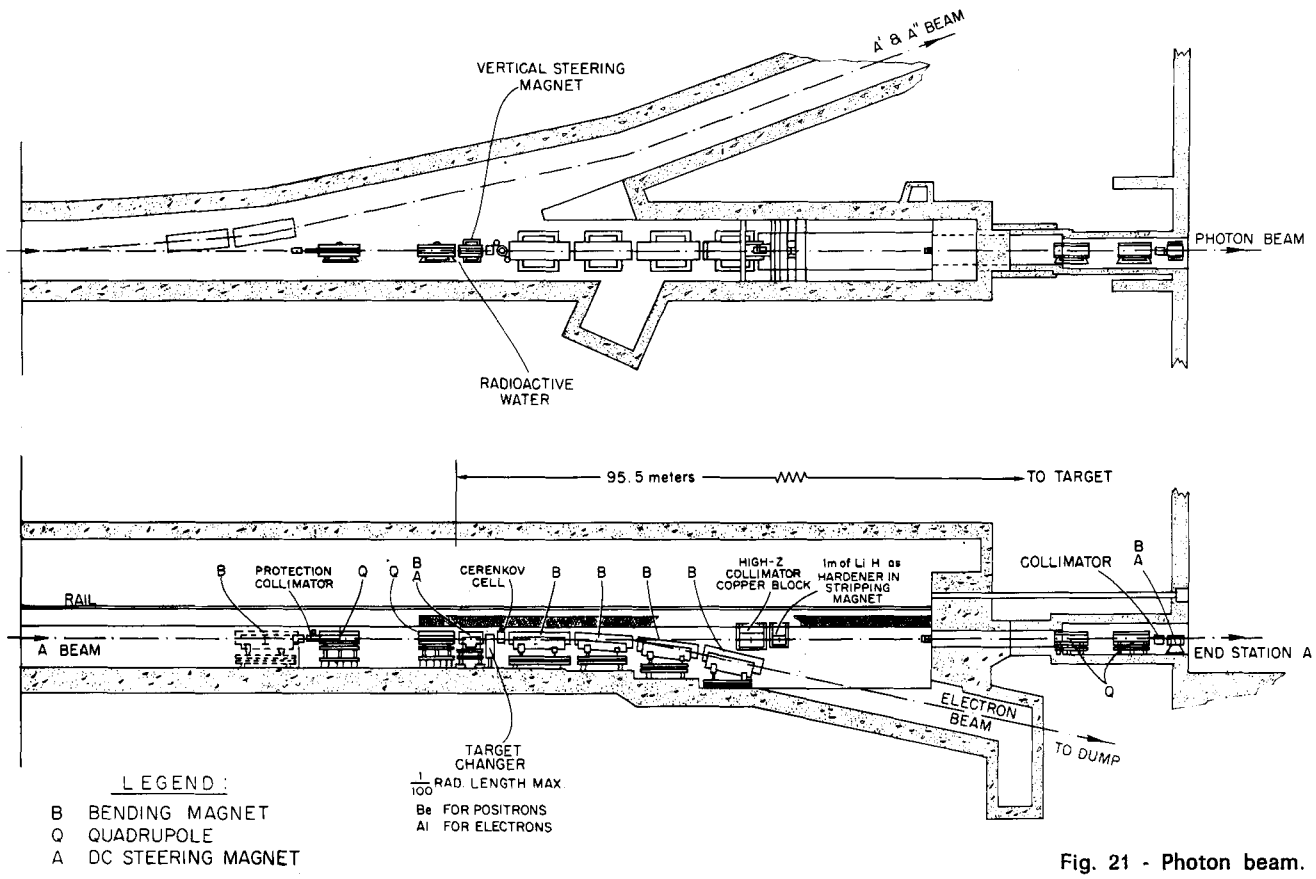

Fig. 21 - Photon beam.

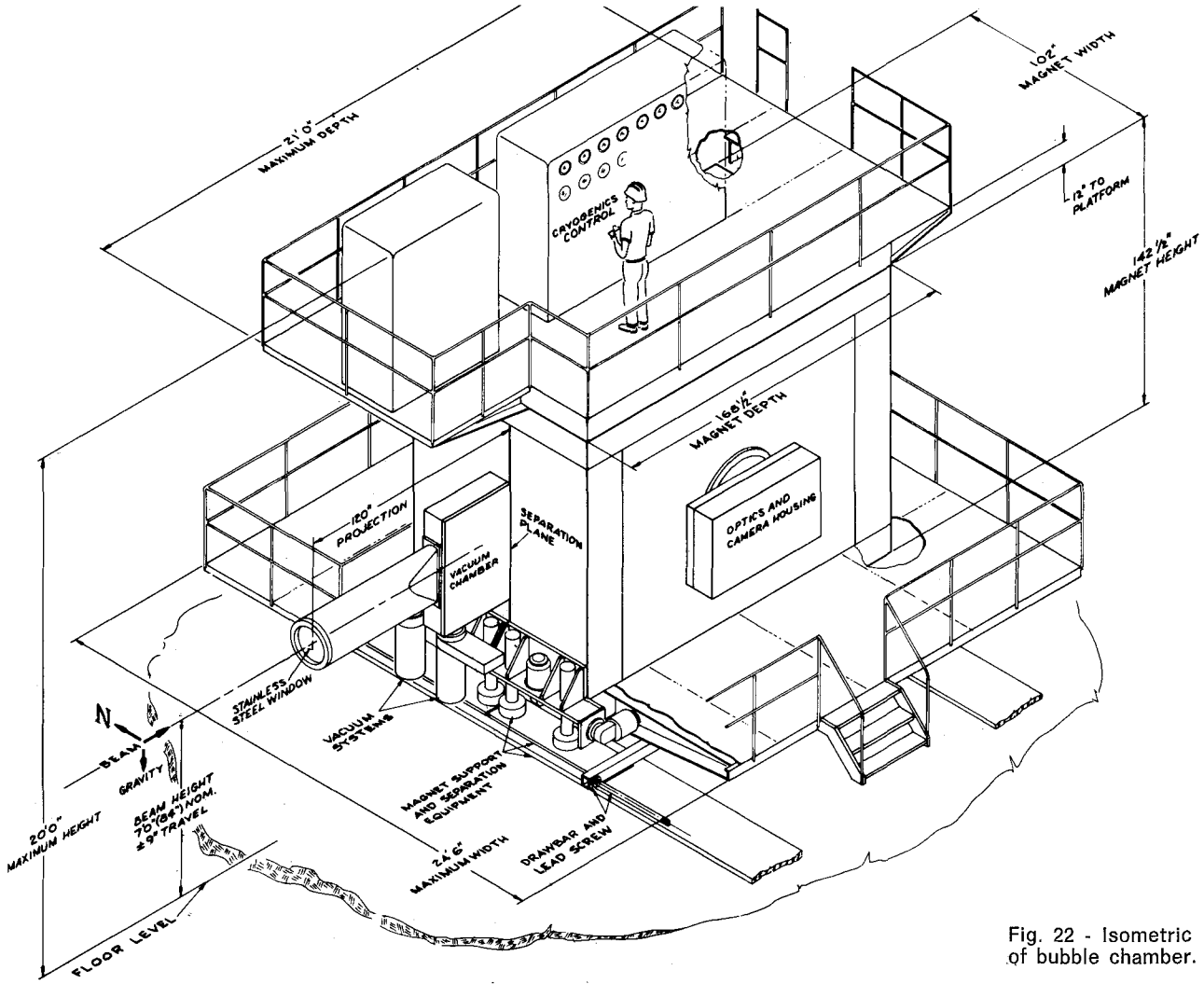

Fig. 22 - Isometric of bubble chamber.

tions. The current was scaled down from 9000 amps.

3. *Photon beam*

A bremsstrahlung beam for use in the large spark chamber and for photoproduction experiments with the two large spectrometers has been designed. A layout of this beam is shown in Fig. 21. As can be seen, it is formed by placing a thin radiator just upstream of the Beam Switchyard dump magnets. The photon beam, which has a shape almost equivalent to the electron beam which produces it, can then be changed in spatial character by the quadrupoles preceding the radiator. In this way a conventional beam of 10^9 equivalent quanta/sec and a weak ribbon beam 1 cm × 30 cm containing $\approx 10^6$ equivalent quanta/sec have been designed. All photon beams will pass through a one-radiation-length lithium hydride hardener.

4. *One meter hydrogen bubble chamber*

This chamber will be used initially to study photoproduction processes with a beam to be described below. Thus, for a reasonably large class of experiments the full-power of the hydrogen bubble chamber technique can be brought to bear on multiparticle final state interactions involving incident photons. The size of the chamber is such that the upper limit for good kinematical analysis is about 8 GeV/c. This, however, is a good match for the monochromatic photon beam in Stage I of SLAC operation.

Typical reactions to be studied are:

$$\gamma + p \rightarrow p + \rho^0$$
$$\rightarrow p + \eta$$
$$\rightarrow p + \omega$$
$$\rightarrow K^+ + \overline{K^0} + p + \pi^-$$

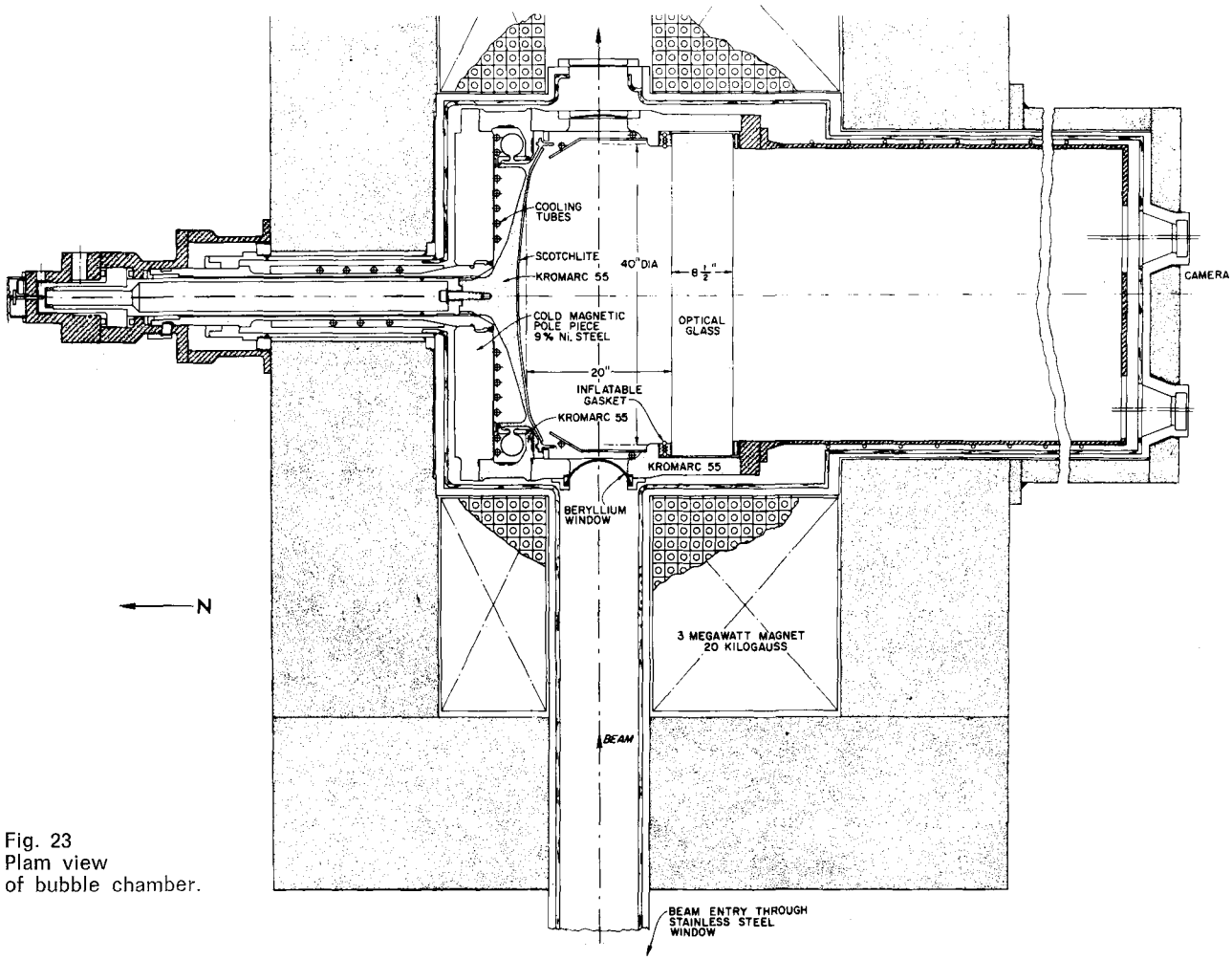

Fig. 23
Plam view
of bubble chamber.

$$\gamma + p \rightarrow \bar{p} + p + p$$
$$\rightarrow \Lambda^\circ + K^\circ + \pi^+ + \pi^- + \pi^+$$

The chamber is designed to pulse twice per second, using a bellows expansion. An isometric drawing is shown in Fig. 22 and a plan view in Fig. 23. It will operate in a magnetic field of 20,000 gauss having a uniformity of ± 2% and radial symmetry. The illumination will be obtained with scotchlite adhered to the moving back plate and ring flash lamps around the lenses. The three views are all on one film strip 70 mm wide. The beam window of the chamber is to be made of beryllium in order to keep the number of electron pairs made in the window to a low value. It is expected that cross sections as low as 10^{-30} cm^2 may be measured in 500,000 picture exposures.

5. *Monochromatic photon beam*

A monochromatic photon beam obtained from observing e^+ e^- annihilation at a fixed angle (16) will be established for the HBC and other detectors. A layout of this beam is shown in Fig. 24. Positrons are brought in to the center of the experimental end station and focused on a thin hydrogen target by the two quadrupoles. The energy of the photon beam can be changed by either varying the energy of the incident positrons or their angle of incidence. The chamber will be placed 60 meters from the target and will have a window large enough to accept something like one-quarter of the produced photons.

6. *Muon beam*

A muon beam from which the pions have been filtered and then momentum-analyzed is also shown in Fig. 24. These muons will be made in a target capable of absorbing as high as 100 kW average electron beam power. At energies between 5 and 15 GeV muon pair production at this beam power gives approximately 10^6 muons/second in a 1% momentum band.

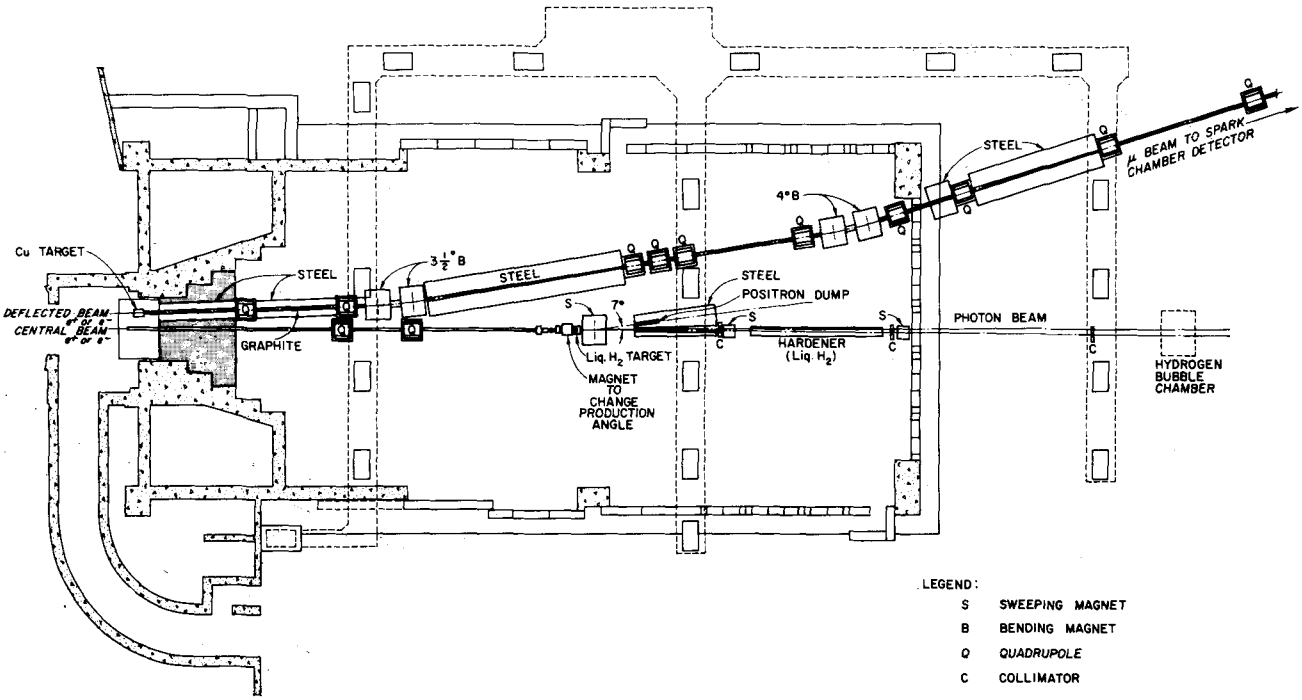

Fig. 24 - Monochromatic and muon beams in end station B.

REFERENCES

(1) R. B. Neal and W. K. H. Panofsky: Proc. Int. Conf. on High Energy Accelerators, Geneva, 1956, vol, I, p. 530.
(2) R. B. Neal: Proc. Int. Conf. on High Energy Accelerators, Geneva, 1959, p. 349.
(3) K. L. Brown, A. L. Eldredge, R. H. Helm, J. H. Jasberg, J. V. Lebacqz, G. A. Loew, R. F. Mozley, R. B. Neal, W. K. H. Panofsky and T. F. Turner: Proc. Int. Conf. on High Energy Accelerators, Brookhaven, 1961, p. 79.
(4) W. K. H. Panofsky: Proc. Int. Conf. on High Energy Accelerators, Dubna, 1963, (Atomizdat, Moscow, 1964) pag. 407.
(5) R. P. Borghi, A. L. Eldredge, G. A. Loew, and R. B. Neal: Design and Fabrication of the Accelerating Structure for the Stanford Two-mile Accelerator, to be published in Advances in Microwaves, vol. I, (Academic Press, New York, N. Y.).
(6) J. V. Lebacqz: Particle Accelerator Conf., Washington, 1965; IEEE Trans. on Nuclear Science, NS-12, No. 3, p. 86 (1965).
(7) C. B. Williams, A. R. Wilmunder, J. Dobson, H. A. Hogg, M. J. Lee, and G. A. Loew: to be published in Proc. of the G-MTT Symposium (IEEE) (held May 5-7, 1965, Clearwater, Florida).
(8) R. H. Miller, R.F. Koontz, and D. D. Tsang: Particle Accelerator Conf., Washington, 1965; IEEE Trans. on Nuclear Science, NS-12 No. 3, p. 804 (1965).
(9) W. B. Herrmannsfeldt: Particle Accelerator Conf., Washington, 1965; IEEE Trans. on Nuclear Science, NS-12, No. 3, p. 929 (1965).
(10) G. A. Loew and R. H. Helm: Particle Accelerator Conf. Washington, 1965; IEEE Trans. on Nuclear Science, NS-12, No. 3, p. 580 (1965).
(11) R.B. Neal: J. Vacuum Sci. Technology (to be published).
(12) S. R. Conviser: Particle Accelerator Conf. Washington, 1965; IEEE Trans. on Nuclear Science, NS-12, No. 3, p. 699 (1965).
(13) W. B. Herrmannsfeldt: Particle Accelerator Conf., Washington, 1965; IEEE Trans. on Nuclear Science, NS-12, No. 3, p. 9 (1965).
(14) R. E. Taylor: Particle Accelerator Conf., Washington, 1965; IEEE Trans. on Nuclear Science, NS-12, No. 3, p. 846 (1965).
(15) W. K. H. Panofsky: Proc. of the Int. Symp. on Electron and Photon Interactions at High Energies, Hamburg, 1965, (to be published).
(16) J. Ballam and Z. Guiragossian: Proc. of the 1964 Conf. on High Energy Physics, Dubna, USSR, (to be published).

DISCUSSION

BLEWETT J. P.: You indicated that the tests on the first two sections resulted in changes in the design of the later sections. Would you say what these changes were?

NEAL: None of the changes which were made changed the fundamental parameters or basic configuration of the accelerator. The accelerator structure itself was not

changed at all, the change of the feed system to compensate for coupler asymmetries having been make prior to the start of the experimental program with the first two sectors. The changes consisted mainly of circuit changes, as for example those made to improve the stability of the microwave phasing system and the r.f. drive system.

LIVINGSTON: Do you plan to use laser light interaction with the main electron beam in order to obtain monochromatic and polarized photons?

NEAL: This technique has been studied extensively and will probably be employed at a later date. However, there are no immediate plans to use this technique in the initial research program. We will start, rather, with the monochromatic photon beam from positron annihilation as discussed earlier.

SCHAFFER: How much additional power will be consumed for focusing the positron beam?

NEAL: Altogheter, approximately 1 megawatt of power is required in the positron source system described. More than one-half of this power is used for focusing.

SCHAFFER: In order to save focusing power for the positron beam a higher r.f. field after the concerter may be of interest in order to apply quadrupole focusing at a minimum distance from the converter. Will a higher number of klystrons per section be used for this purpose?

NEAL: Yes. We will use the entire power output from a single klystron to provide power to the accelerator section immediately downstream of the positron source. This is in contrast to the distribution of power along most of the accelerator length where the power from each klystron is split four ways and is used to power four successive 10 foot accelerator sections.

AMMAN: Which is the electron energy at the converter?

NEAL: The energy will be approximately 5 GeV.

AMMAN: Can you give some details on the Cerenkov monitors for beam prcfile?

NEAL: The Cerenkov type of beam profile monitor consists of a piece of quartz about 0.030" thick which can be inserted into the beam and removed by the operator. The Cerenkov radiation is observed by a radiation-resistant television set. No attempt is made to use the beam after it passes through the quartz; the device is removed after the profile has been viewed. A gas-filled Cerenkov profile monitor for use in the SLAC beamswitchgard will be described by Neet in a separate paper.

AMMAN: My third question is related to what has been said by Salvini: is there any design of a primary beam stretcher or muon ring at SLAC?

NEAL: A muon ring has been studied by Tinlot of the University of Rochester and was reported on at the Washington Conference in February, 1965. No formal proposal for such a storage ring has been submitted.

GITTELMAN: There is a study being made by a group from Rochester of a muon (and antiproton) storage ring of the type described by Salvini. The SLAC linac will be used as the first stage of the injector?

NEAL: Refer to answer to question by Amman.

THE 360 MEV TRAVELING-WAVE LINEAR ACCELERATOR

A. K. Valter, I. A. Grishaev, L. A. Makhnenko, G. K. Demianenko, A. I. Zykov, G. M. Ivanov, K. S. Rubtzov and V. A. Skubko.

Phisical-Tecnical Institute, Academy of Sciences, Kharkov (USSR)

(Presented by I. A. Grishaev)

Main technical characteristics and some results of 360 MeV accelerators research have been published before (1). More details study data of accelerating systems are presented in this report. Arrangements for improvements on radial-angle characteristics of the electron beam are considered. A brief survey on an exploitation test of the accelerator is given.

I. DETERMINATION OF ACCELERATING SYSTEM ELECTRODYNAMICS PARAMETERS

1. From first accelerator research results (1), one can see that calculated parameters of the accelerating system differ from experimental ones. If the calculated accuracy of the resonant frequency is not below 0,1% (it is quite satisfactorily), a determination error of the electrical field